

# Low-loss plasmonic metamaterial based on epitaxial gold monocrystal film

V. A. Fedotov,<sup>1,2,\*</sup> T. Uchino,<sup>2,3,4</sup> and J. Y. Ou<sup>1,2</sup>

<sup>1</sup>*Optoelectronics Research Centre, University of Southampton, SO17 1BJ, UK*

<sup>2</sup>*Centre for Photonic Metamaterials, University of Southampton, SO17 1BJ, UK*

<sup>3</sup>*School of Electronics and Computer Science, University of Southampton, SO17 1BJ, UK*

<sup>4</sup>*Department of Electronics and Intelligent Systems, Tohoku Institute of Technology, 982-8577, Japan*  
\*[vaf@orc.soton.ac.uk](mailto:vaf@orc.soton.ac.uk)

**Abstract:** We demonstrate high-finesse plasmonic metamaterial with strong resonant response in the near-IR spectral range fabricated using a thin low-loss film of gold monocrystal. The monocrystal was grown using specially formulated simplified crystal growth procedure based on epitaxial deposition, which makes it readily accessible to both plasmonics and metamaterials communities.

©2012 Optical Society of America

**OCIS codes:** (160.3918) Metamaterials; (310.6628) Subwavelength structures, nanostructures; (250.5403) Plasmonics.

---

## References and links

1. V. G. Veselago and E. E. Narimanov, "The left hand of brightness: past, present and future of negative index materials," *Nat. Mater.* **5**(10), 759–762 (2006).
2. N. I. Zheludev, "Applied physics. The road ahead for metamaterials," *Science* **328**(5978), 582–583 (2010).
3. D. A. Bobb, G. Zhu, M. Mayy, A. V. Gavrilenko, P. Mead, V. I. Gavrilenko, and M. A. Noginov, "Engineering of low-loss metal for nanoplasmonic and metamaterials applications," *Appl. Phys. Lett.* **95**(15), 151102 (2009).
4. M. G. Blaber, M. D. Arnold, and M. J. Ford, "Optical properties of intermetallic compounds from first principles calculations: a search for the ideal plasmonic material," *J. Phys. Condens. Matter* **21**(14), 144211 (2009).
5. A. Boltasseva and H. A. Atwater, "Materials science. Low-loss plasmonic metamaterials," *Science* **331**(6015), 290–291 (2011).
6. M. A. Noginov, G. Zhu, M. Mayy, B. A. Ritzo, N. Noginova, and V. A. Podolskiy, "Stimulated emission of surface plasmon polaritons," *Phys. Rev. Lett.* **101**(22), 226806 (2008).
7. E. Plum, V. A. Fedotov, P. Kuo, D. P. Tsai, and N. I. Zheludev, "Towards the lasing spaser: controlling metamaterial optical response with semiconductor quantum dots," *Opt. Express* **17**(10), 8548–8551 (2009).
8. S. M. Xiao, V. P. Drachev, A. V. Kildishev, X. J. Ni, U. K. Chettiar, H. K. Yuan, and V. M. Shalaev, "Loss-free and active optical negative-index metamaterials," *Nature* **466**(7307), 735–738 (2010).
9. M. Kuttge, E. J. R. Vesseur, J. Verhoeven, H. J. Lezec, H. A. Atwater, and A. Polman, "Loss mechanisms of surface plasmon polaritons on gold probed by cathodoluminescence imaging spectroscopy," *Appl. Phys. Lett.* **93**(11), 113110 (2008).
10. A. Green, E. Bauer, R. L. Peck, and J. Dancy, "Stages of epitaxial film formation," *Krist. Tech.* **5**(3), 345–366 (1970).
11. B. Lewis, "Physical processes in epitaxial growth," *Thin Solid Films* **7**(3-4), 179–217 (1971).
12. K. M. Kunz, A. K. Green, and E. Bauer, "On the formation of single crystal films of F.C.C. metals on alkali halide cleavage planes in ultrahigh vacuum," *Phys. Status Solidi* **18**(1), 441–457 (1966).
13. D. J. Stirland, "Electron-bombardment-induced changes in the growth and epitaxy of evaporated gold films," *Appl. Phys. Lett.* **8**(12), 326–328 (1966).
14. W. A. Jesser and J. W. Matthews, "Growth of copper, silver, and gold on twelve Alkali halides cleaved in vacuum," *J. Cryst. Growth* **5**(2), 83–89 (1969).
15. Model SPEC. SOU/150103/TPG, capable of depositing thin multi-layers of metallic and dielectric layers (specially customized for University of Southampton).
16. N. W. Ashcroft and N. D. Mermin, *Solid State Physics*, 7th ed. (Wiley, New York, 1996).
17. A. R. West, *Basic Solid State Chemistry* (Wiley, New York, 1994).
18. M. Hegner, P. Wagner, and G. Semenza, "Ultralarge atomically flat template-stripped Au surfaces for scanning probe microscopy," *Surf. Sci.* **291**(1-2), 39–46 (1993).
19. M. Kuttge, E. J. R. Vesseur, J. Verhoeven, H. J. Lezec, H. A. Atwater, and A. Polman, "Loss mechanisms of surface plasmon polaritons on gold probed by cathodoluminescence imaging spectroscopy," *Appl. Phys. Lett.* **93**(11), 113110 (2008).
20. V. P. Drachev, U. K. Chettiar, A. V. Kildishev, H. K. Yuan, W. Cai, and V. M. Shalaev, "The Ag dielectric function in plasmonic metamaterials," *Opt. Express* **16**(2), 1186–1195 (2008).

21. J. N. Hilfiker, N. Singh, T. Tiwald, D. Convey, S. M. Smith, J. H. Baker, and H. G. Tompkins, "Survey of methods to characterize thin absorbing films with spectroscopic ellipsometry," *Thin Solid Films* **516**(22), 7979–7989 (2008).
22. N. P. Blanchard, C. Smith, D. S. Martin, D. J. Hayton, T. E. Jenkins, and P. Weightman, "High-resolution measurements of the bulk dielectric constants of single crystal gold with application to reflection anisotropy spectroscopy," *Phys. Status Solidi, C Conf. Crit. Rev.* **0**(8), 2931–2937 (2003).
23. D. W. Lynch and W. R. Hunter, "Comments on the optical constants of metals and an introduction to the data for several metals," in *Handbook of Optical Constants of Solids*, E.D. Palik, ed. (Academic, Orlando, Fla., 1985).
24. P. B. Johnson and R. W. Christy, "Optical constants of noble metals," *Phys. Rev. B* **6**(12), 4370–4379 (1972).
25. V. A. Fedotov, M. Rose, S. L. Prosvirnin, N. Papasimakis, and N. I. Zheludev, "Sharp trapped-mode resonances in planar metamaterials with a broken structural symmetry," *Phys. Rev. Lett.* **99**(14), 147401 (2007).
26. N. Papasimakis, V. A. Fedotov, Y. H. Fu, D. P. Tsai, and N. I. Zheludev, "Coherent and incoherent metamaterials and order-disorder transitions," *Phys. Rev. B* **80**(4), 041102 (2009).
27. V. A. Fedotov, N. Papasimakis, E. Plum, A. Bitzer, M. Walther, P. Kuo, D. P. Tsai, and N. I. Zheludev, "Spectral collapse in ensembles of metamolecules," *Phys. Rev. Lett.* **104**(22), 223901 (2010).
28. N. Papasimakis and N. I. Zheludev, "Metamaterial-induced transparency," *Opt. Photon. News* **20**(10), 22–27 (2009).
29. N. Papasimakis, V. A. Fedotov, N. I. Zheludev, and S. L. Prosvirnin, "Metamaterial analog of electromagnetically induced transparency," *Phys. Rev. Lett.* **101**(25), 253903 (2008).
30. A. E. Nikolaenko, F. De Angelis, S. A. Boden, N. Papasimakis, P. Ashburn, E. Di Fabrizio, and N. I. Zheludev, "Carbon nanotubes in a photonic metamaterial," *Phys. Rev. Lett.* **104**(15), 153902 (2010).
31. N. I. Zheludev, S. L. Prosvirnin, N. Papasimakis, and V. A. Fedotov, "Lasing spaser," *Nat. Photonics* **2**(6), 351–354 (2008).
32. E. Plum, K. Tanaka, W. T. Chen, V. A. Fedotov, D. P. Tsai, and N. I. Zheludev, "A combinatorial approach to metamaterials discovery," *J. Opt.* **13**(5), 055102 (2011).
33. I. M. Pryce, K. Aydin, Y. A. Kelaita, R. M. Briggs, and H. A. Atwater, "Highly strained compliant optical metamaterials with large frequency tunability," *Nano Lett.* **10**(10), 4222–4227 (2010).
34. H. H. Li, "Refractive index of alkali halides and its wavelength and temperature derivatives," *J. Phys. Chem. Ref. Data* **5**(2), 329–349 (1976).
35. P. Nagpal, N. C. Lindquist, S. H. Oh, and D. J. Norris, "Ultrasoft patterned metals for plasmonics and metamaterials," *Science* **325**(5940), 594–597 (2009).

Metamaterials are a class of artificial materials designed to interact with light in ways no natural materials can [1, 2]. The exotic and often dramatic physics demonstrated by the metamaterials is generally underpinned by the light-scattering properties of sub-wavelength metallic resonators (metamolecules) that form metamaterials. Due to its resonant nature the response of the metamaterials is very sensitive to the presence of dissipative losses in the constituting metals. The losses are particularly strong in the plasmonic regime (i.e. at optical frequencies) hampering the use of metamaterials for photonic applications. The list of mainstream solutions considered at present includes, in particular, the search for better plasmonic media among metallic alloys, semiconductors and conductive oxides [3–5], as well as direct compensation of losses by combining metamaterials with various optical gain media [6–8]. Those solutions, however, aim to eliminate (or minimise) Joule losses, while in practice dissipation rates are often much higher than expected from the Ohm's law alone. The additional significant contribution comes from surface roughness and grain boundary scattering due to polycrystalline nature of evaporated/sputtered metal films [9], and therefore switching to monocrystals of noble metals should alone provide a substantial mileage in reducing plasmonic losses.

In this paper we describe an extremely simple and robust crystal growth technique, which yields very thin large area single-crystal films of gold ideally suited for hosting high-finesse plasmonic metamaterials. We confirmed the exceptional quality of the grown monocrystal by fabricating a nanostructured metamaterial with a complex asymmetric pattern, which exhibits sub-radiant high - Q resonance in the near-IR spectral range.

Our crystal growth technique is based on epitaxial deposition, where metal vapour condenses on a crystalline substrate to a film with crystallite orientations closely related to that of the substrate. Although large gold monocrystals can also be grown using the Czochralski process, they are usually difficult to obtain in the form of a thin film and therefore can be seldom considered for metamaterial and plasmonic device fabrication. In the past, epitaxial growth of gold and other f.c.c. metals was demonstrated and thoroughly investigated for alkali-halide cubic crystals NaCl and KCl [10, 11]. In most of the cases,

however, the growing procedure was complicated by the requirement of contaminating gases [12] or electron irradiation of the substrate [13], and often produced gold and silver films with (111) fibre texture [12, 14].

We have revisited the epitaxial growth techniques and found a combination of a substrate and deposition conditions that substantially simplified the procedure of growing gold monocrystals. As a substrate we used lithium fluoride (LiF). This ionic crystal has a face centred cubic lattice with the constant of 4.03 Å, which implies virtually no mismatch with the lattices of gold (less than 1.5%) and therefore results in a low interfacial energy for the parallel orientation of the gold film. Furthermore, LiF is highly transparent dielectric with an exceptionally broad transmission window spanning from VUV to mid-IR (0.15 to 6 μm), and one of few hard and non-hygroscopic alkali-halide crystals, which makes it the ideal substrate for hosting metamaterial-based optical devices. A suitable (100) slab of LiF was obtained by cleaving the crystal with a razor blade immediately before placing it in the high-vacuum sputtering chamber (Kurt J. Lesker sputter deposition system [15]), where the slab was kept at 460C during the deposition. Gold was deposited at the rate of 0.22 nm/sec and base pressure of  $5 \times 10^{-6}$  mbar using DC regime of the sputtering system. The sputtering produced an 80 nm thick continuous and atomically smooth film of a gold monocrystal with (100) domain orientation. That was confirmed with scanning electron and atomic force microscopy, and x-ray diffractometry (see Figs. 1(a), 1(b) and 1(c)). The lattice constants of gold and LiF estimated from the positions of the diffraction peaks were 4.11 Å and 4.03 Å and agreed well with the reference data [16, 17]. The gold film had remarkably small RMS roughness of 0.2 nm, which is comparable to that of the template-stripped gold surfaces [18], and is almost an order of magnitude smaller than RMS roughness of polycrystalline films produced by fast sputtering [19, 20]. Post-deposition test annealing at 550C induced no change in the morphology of the film and therefore was omitted during preparation of the samples.

We also determine complex dielectric constant of the film using ellipsometry in 200 – 1700 nm range of wavelengths (J. A. Wollam VASE). The real and imaginary parts of the dielectric constant were retrieved through the direct inversion of  $\Psi$  and  $\Delta$ , which is known to work well for opaque films with negligible surface roughness [21].  $\Psi$  and  $\Delta$  were measured for two different areas of the sample and incidence angles of 70°, 75° and 80°. We compared our results with the reference data available for bulk [22] and thin film [23] gold monocrystals, as well as fast evaporated polycrystalline films [24]. Our results showed a remarkable agreement with both sets of monocrystal data for real and, most importantly, imaginary part of the dielectric constant, which characterizes the level of plasmonic losses in the metal (see Fig. 1(d)). A pronounced deviation from the polycrystalline data in the UV and near-IR could not be attributed to the instrumental error, indicating on a genuine difference between the optical properties of evaporated and epitaxially grown films.

We argue that such a thin film of gold monocrystal presents an ideal base for fabricating high-quality plasmonic metamaterials with a well-predicted optical response: (i) its plasmonic losses do not exceed the Ohm's law limit; it enables to attain much better control over the nano-patterning process, as it is structurally ordered and naturally harder than its polycrystalline counterparts. To demonstrate the full potential of the film we fabricated a complex plasmonic metamaterial with a known, strong resonance located in the near-IR spectral range, where Drude-like electronic properties of gold are not affected by the inter-band transition. Also, comparing the response of the fabricated metamaterial with the theoretical prediction would enable to judge on the adequateness of the film's dielectric function extracted from our ellipsometric measurements.

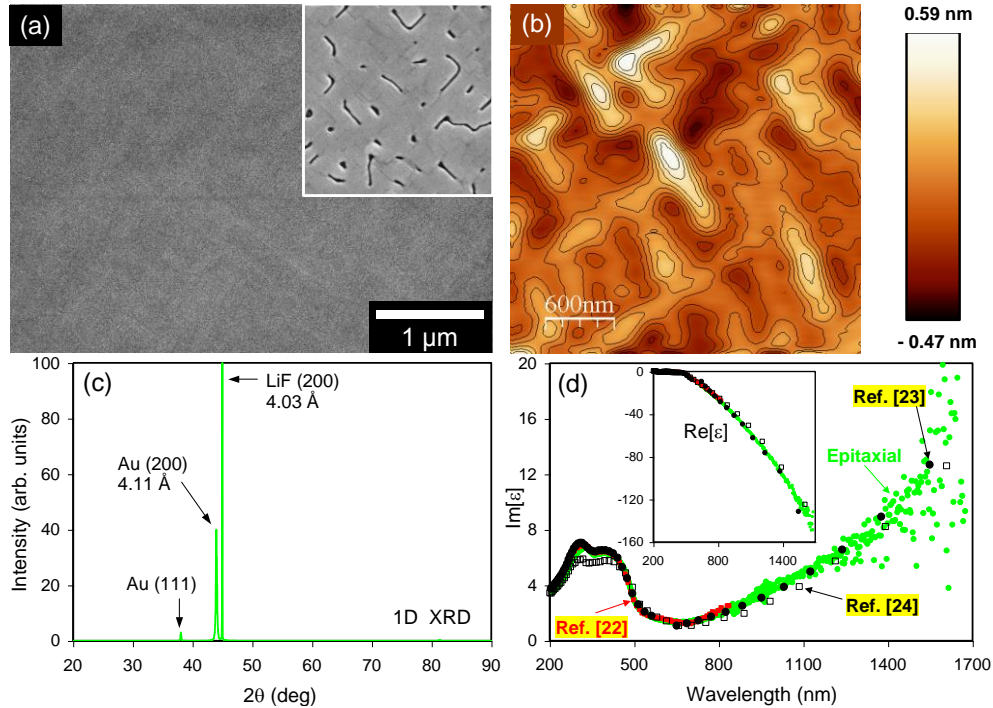


Fig. 1. Gold film epitaxially grown on LiF. (a) Scanning electron microscope image of the film. Inset shows the signs of crystalline structure observed in the film at an early stage of deposition: the film is seen to grow from cubic islands with some gaps and stitches appearing along  $\langle 100 \rangle$  directions. (b) Surface roughness of the film imaged with an atomic force microscope. Colours show amplitude of the height fluctuations. (c) 1D x-ray diffraction pattern of gold film/LiF with (200) peaks. A small peak at  $38^\circ$  is associated with (111) reflection of gold film, and is due to imperfect condensation on the facet. (d) Imaginary part of the dielectric constant of gold as a function of wavelength. Green circles show values retrieved for the epitaxially grown film using spectroscopic ellipsometry (large point spread above 1300 nm is due to reduced sensitivity of our spectrometer in the near-IR). The reference data are represented by red squares (bulk single crystal [22]), black circles (thin film with large monocrystal domains [23]) and black open squares (polycrystalline thin film [24]). Inset shows the measured and reference data for the real part of the dielectric constant.

The metamaterial pattern was based on the array of asymmetrically split rings (ASR) originally exploited in high-Q microwave metamaterials exhibiting sharp sub-radiant resonances of Fano type [25]. Those metamaterials belong to important classes of coherent [26, 27] and EIT-like artificial media [28] with an identified potential to slow light [29], enhance optical nonlinearities [30] and produce low-dimensional plasmon-fuelled coherent light source, the lasing spaser [31]. Due to its sub-radiant nature the resonant response of such structures is very sensitive to the pattern defects and especially dissipation in the metal, and therefore manufacturing optical metamaterials operating close to the theoretical limit has so far been extremely challenging. Also, in the previous fabrication attempts the circular elements of ASR-pattern were replaced with square ones composed of straight segments [32, 33], a simplification generally better suited to the nano-fabrication process but leading to additional plasmonic losses at sharp corners.

Here we have fully reproduced the shape of the microwave pattern on the nano-scale with the scaling ratio of about 47000: 1 (see Fig. 2(a)). The pattern was milled in the gold film using 55 nC/cm ion beam focused to a  $20^\circ$  cone (Helios Nanolab 600), which produced a negative version of ASR-metamaterial with the split rings defined by 40 nm wide circular slits (apertures). The rings had the diameter of 240 nm and were spaced 320 nm apart. The asymmetry of the pattern was optimised to yield a strong resonant response in the telecom

range 1.3 – 1.5  $\mu\text{m}$ : the two arcs of the split rings were 180° and 130° long and separated by equal splits of 25°. The metamaterial sample contained over 5000 sub-wavelength split ring resonators (*size/wavelength ratio is less than 1/4*) covering the area of about 23  $\mu\text{m}$  x 23  $\mu\text{m}$ . The micrograph of the sample taken with scanning electron microscope (see Fig. 2(a)) demonstrates excellent fidelity of the fabricated structure, where every split-ring nano-aperture featured uniform slit width and was the exact copy of its neighbours in the array. Importantly, we did not observe any random pattern distortions and slit defects due to re-deposition and ion-beam exposure variations that are commonly encountered in the case of polycrystalline films.

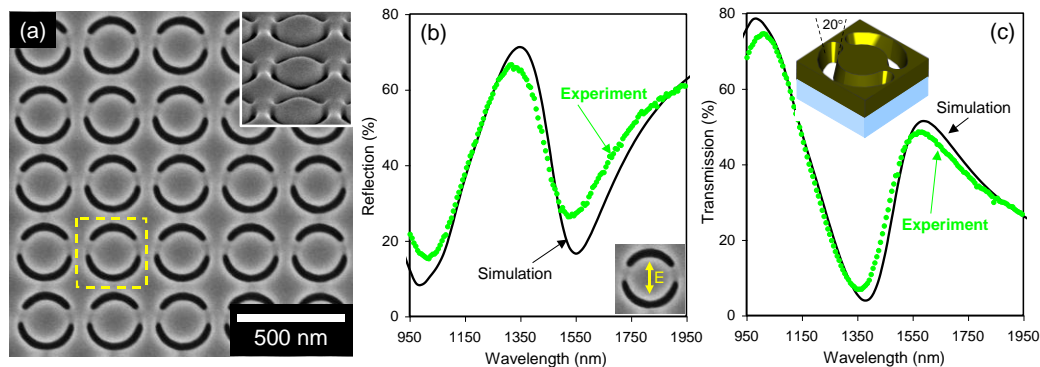


Fig. 2. High-finesse infrared plasmonic metamaterial. (a) Scanning electron microscope image of complex asymmetrically-split ring pattern milled in epitaxial gold film. Yellow dashed box indicates elementary unit cell of the periodic pattern (*size/wavelength ratio is less than 1/4*). Inset shows 3D view of the milled structure. (b) Reflection spectra of the plasmonic metamaterial. Green circles show experimentally measured values, while black curve represents the result of simulation. Inset shows orientation of incident polarization with respect to the metamaterial pattern. (c) Transmission spectra of the plasmonic metamaterial. Green circles show experimentally measured values, black curve - result of simulation. Inset shows the model of the structure's unit cell used in simulations.

The reflection and transmission spectra of our metamaterial measured with linearly polarized light (CRAIC QDI-2010 equipped with a Glan-Thompson prism) are shown in Figs. 2(b) and 2(c) for 0.95 – 1.95  $\mu\text{m}$  range of wavelengths. Its sub-radiant resonance can be seen at around 1.35  $\mu\text{m}$ . The resonance results from anti-symmetric dipolar excitations of the opposite arcs in each asymmetrically-split ring [25] and, following the Babinet's principle, appears as a peak in reflection and dip in transmission for the incident polarization parallel to the ring's symmetry axis (as indicated in the inset to Figs. 2(b)). The plots reveal strong resonant behaviour of the fabricated metamaterial with large variations in the magnitude of its spectral response (more than 40% peak-to-peak) and the corresponding quality factor  $Q$  of around 4.

We also compared the experimental data with the results of rigorous calculations performed with finite element modelling software COMSOL. Our model reproduced all features of the metamaterial pattern and their dimensions exactly and even took into account gradual widening of the slit's width towards the gold-air interface that resulted naturally from focussed ion milling (see inset to Fig. 2(c)). The dispersion of the dielectric constant of gold monocrystal in our model was taken from tabulated data [23], while dielectric constant of LiF was 1.91 [34] and assumed constant in the 0.95 – 1.95  $\mu\text{m}$  range of wavelengths. As one can see from Figs. 2(b) and 2(c), the experiment and simulation are in a very good agreement both in terms the magnitude of transmission/reflection and spectral location of the resonance, thus confirming an exceptional quality of the fabricated metamaterial with the level of plasmonic losses little affected by the nano-patterning. A small mismatch between the measured and simulated reflection spectra we attribute to the complex topology of the structure's gold-air

interface resulted from FIB-induced re-deposition (see inset to Fig. 2(a)) and the parasitic losses introduced through gallium ion implantation, as suggested in [35].

In conclusion, we have identified a very simple and robust epitaxial growth technique that yields large-area thin films of single-crystal gold ideally suited for the fabrication of high-quality metamaterials. Plasmonic losses here are capped only by the Ohm's law thus lowering the pump levels that would normally be required for loss compensation and lasing in gain-assisted metamaterials. Another very important advantage offered by epitaxial films is that they are ordered and naturally harder than their polycrystalline counterparts, and therefore enable to retain the full control over the nanofabrication process making it possible to produce very complex high-finesse metamaterial and plasmonic structures and circuits. With slight adjustment of the control parameters the epitaxial growth technique can also be employed for depositing monocrystals of other common plasmonic metals, such as aluminium, copper and silver, which all have their lattice constants similar to that of gold.

### **Acknowledgments**

The authors would like to acknowledge Dr. Kevin MacDonald and Prof. Nikolay Zheludev for their help with preparing the manuscript and AFM imaging, as well as EPSRC (UK) for the financial support through the Career Acceleration Fellowship and Programme Grant.